







ORIGINAL RESEARCH

Inhibition of miR-155 Attenuates Detrimental Vascular Effects of Tobacco Cigarette Smoking

Giacomo Frati, MD*¹; Maurizio Forte, PhD*¹; Flavio di Nonno, MS; Antonella Bordin, PhD; Isotta Chimenti, PhD; Vittorio Picchio, PhD; Elena Cavarretta , MD, PhD; Rosita Stanzione, MS; Franca Bianchi, MS; Roberto Carnevale , PhD; Cristina Nocella, PhD; Sonia Schiavon , MS; Daniele Vecchio , MS; Simona Marchitti , MS; Elena De Falco, PhD; Speranza Rubattu, MD; Francesco Paneni, MD, PhD; Giuseppe Biondi-Zoccai, MD; Francesco Versaci, MD; Massimo Volpe, MD; Francesca Pagano, PhD[†]; Sebastiano Sciarretta , MD, PhD[†]

BACKGROUND: The role of microRNAs dysregulation in tobacco cigarette smoking–induced vascular damage still needs to be clarified. We assessed the acute effects of tobacco cigarette smoking on endothelial cell-related circulating microRNAs in healthy subjects. In addition, we investigated the potential role of microRNAs in smoking-dependent endothelial cell damage.

METHODS AND RESULTS: A panel of endothelial-related microRNAs was quantified in healthy subjects before and after smoking 1 tobacco cigarette. Serum levels of miR-155 were found to be significantly increased shortly after smoking. We also observed a progressive and significant miR-155 accumulation in culture media of human endothelial cells after 30 minutes and up to 4 hours of cigarette smoke condensate treatment in vitro without evidence of cell death, indicating that miR-155 can be released by endothelial cells in response to smoking stress. Cigarette smoke condensate appeared to enhance oxidative stress and impair cell survival, angiogenesis, and NO metabolism in human endothelial cells. Notably, these effects were abrogated by miR-155 inhibition. We also observed that miR-155 inhibition rescued the deleterious effects of cigarette smoke condensate on endothelial-mediated vascular relaxation and oxidative stress in isolated mouse mesenteric arteries. Finally, we found that exogenous miR-155 overexpression mimics the effects of smoking stress by inducing the upregulation of inflammatory markers, impairing angiogenesis and reducing cell survival. These deleterious effects were associated with downregulation of vascular endothelial growth factor and endothelial NO synthetase.

CONCLUSIONS: Our results suggest that miR-155 dysregulation may contribute to the deleterious vascular effects of tobacco smoking.

Key Words: cardiovascular diseases ■ cigarette smoking ■ endothelial dysfunction ■ microRNAs ■ miR-155

Cardiovascular diseases still represent the most common cause of death in Western countries.¹ Among cardiovascular risk factors, tobacco smoking is one of the most relevant² and is dramatically associated with adverse cardiovascular events

and cardiac death.³ It also promotes the onset of other cardiovascular risk factors, such as hypertension, atherosclerosis, and coronary heart diseases, thereby further increasing patient global risk profile.^{2,4} Mechanistically, cigarette smoking directly

Correspondence to: Sebastiano Sciarretta, MD, PhD, Department of Medical-Surgical Sciences and Biotechnologies, Sapienza University of Rome, Latina, Italy. E-mail: sebastiano.sciarretta@uniroma1.it

Supplementary Material for this article is available at <https://www.ahajournals.org/doi/suppl/10.1161/JAHA.120.017000>

*Drs Frati and Forte contributed equally to this work.

[†]Drs Pagano and Sciarretta are co-senior authors.

For Sources of Funding and Disclosures, see page 11.

© 2020 The Authors. Published on behalf of the American Heart Association, Inc., by Wiley. This is an open access article under the terms of the Creative Commons Attribution-NonCommercial-NoDerivs License, which permits use and distribution in any medium, provided the original work is properly cited, the use is non-commercial and no modifications or adaptations are made.

JAHA is available at: www.ahajournals.org/journal/jaha

CLINICAL PERSPECTIVE

What Is New?

- Circulating serum levels of miR-155 increase after smoking 1 cigarette in healthy subjects.
- Inhibition of miR-155 rescues the detrimental effects of smoking stress on endothelial function in vitro and ex vivo.

What Are the Clinical Implications?

- miR-155 may represent a valid biomarker for cardiovascular risk stratification of subjects who smoke.

Nonstandard Abbreviations and Acronyms

| | |
|---------------|--|
| CSC | cigarette smoke condensate |
| HUVECs | human umbilical vein endothelial cells |

increases oxidative stress in endothelial cells, leading to endothelial dysfunction that represents the main pathophysiological substrate underlying the development and progression of cardiovascular diseases.^{5,6} However, the molecular mechanisms promoting the harmful effects of cigarette smoking on endothelial function still need to be fully clarified. The elucidation of this aspect would be useful to develop new cardiovascular preventive strategies in subjects who smoke.

MicroRNAs are endogenous, small noncoding RNAs involved in the regulation of gene expression. They act as key regulators of several cellular processes, such as cell proliferation, death, differentiation, and intercellular communication.⁷ It was demonstrated that circulating microRNAs contribute to the genesis and progression of vascular damage in response to stress.⁸ Moreover, microRNAs also emerged as important predictors for cardiovascular diseases.^{9–11} In this regard, different microRNAs were reported to be highly expressed in the blood of patients with acute myocardial infarction and to represent potential diagnostic and prognostic biomarkers in patients with coronary artery diseases.^{12–15}

Dysregulation of circulating microRNAs was also found in the presence of main cardiovascular risk factors, such as diabetes mellitus, hypertension, and cardiac hypertrophy.^{16–18} However, the impact of acute tobacco smoking on circulating microRNAs and the possible role of microRNA in smoking-induced endothelial damage are still not fully understood. In this study, we investigated the potential role of microRNA

deregulation induced by smoke on endothelial cells and mouse vessels.

METHODS

The data that support the findings of this study are available from the corresponding author upon reasonable request.

Patient Sample Collection and Experimental Design

Subject recruitment, participant characteristics, and experimental procedures were previously reported by Carnevale et al.⁶ In summary, serum samples for microRNA level evaluations were collected from 40 healthy young (21 women, mean age 28±5.3) non-smoker (n=20) and smoker (n=20) participants, free of any disease, just before and within 30 minutes after smoking 1 tobacco cigarette with a mean nicotine content of 0.6 mg according to the package label. Participants enrolled in the study gave informed consent prior to their inclusion. The protocol was approved by the local ethical committee and was performed in compliance with the Declaration of Helsinki.

RNA Extraction and MicroRNA Quantification

Endothelial-related microRNAs, based on the available literature (Table S1), were quantified in cells as well as fluids (serum and cell culture supernatants). Fluid samples were centrifuged at 25 000g to remove debris, platelets, or cells, and RNA was extracted from 200 µL of serum/conditioned media using the Qiagen miRNeasy kit (Qiagen GmbH, Hilden, Germany) following the manufacturer's instructions with further modifications. Syn-cel-miR-39 spike in synthetic RNA (Qiagen GmbH) was added to monitor extraction efficiency and to normalize microRNA levels. miR-155 levels were quantified using absolute quantification. A standard curve was generated with a synthetic miR-155 RNA, and the copy number was determined according to the standard curve. Cellular RNA was extracted using the Qiagen miRNeasy kit following the standard procedure. The expression of microRNAs was assessed by real-time quantitative polymerase chain reaction using the Taqman microRNA assays as described elsewhere.¹⁹ Relative microRNA expression in vitro was calculated using small nuclear RNA (snRNA-U6) as endogenous control with the comparative $2^{-\Delta\Delta Ct}$ method.²⁰

Cell Cultures and Treatments

Cigarette smoke condensate (CSC) was purchased by Murty Pharmaceuticals (Lexington, KY) (stock

solution 40 mg/mL in DMSO) and diluted in cell medium at the final concentration of 20 µg/mL, based on previous studies.^{21–23} Human umbilical vein endothelial cells (HUVECs) (Lonza, Monza, Italy) were grown in EGM2 (Lonza) complete medium in a humidified incubator at 37°C and 5% CO₂. For CSC and H₂O₂ experiments, HUVECs were serum starved for 4 hours using DMEM low-glucose medium (Lonza). The medium was then changed with DMEM low-glucose medium containing 20 µg/mL CSC or 100 µmol/L H₂O₂. Cells incubated in DMEM low-glucose medium with vehicle (DMSO <0.01%) were used as controls. HUVECs were harvested after 15 minutes, 30 minutes, 1 hour, 4 hours, and 12 hours of treatment (t=0). Cells between passages 2 and 4 were used for all the experiments.

Apoptosis

Apoptosis in CSC-treated or H₂O₂-treated HUVECs and respective control cells was evaluated by the Annexin V-FITC Apoptosis detection kit (eBioscience, San Diego, CA) according to the manufacturer's protocol modified for adherent cells.²⁴ Data were collected using fluorescence-activated cell sorting (FACS) Calibur flow cytometer (BD Biosciences, San Jose, CA) and analyzed using FlowJo software (FlowJo LLC, Ashland, OR).

miR-155 Mimic Transfection in HUVECs

Transient transfection of miR-155 mimic (Sigma Aldrich-Merck, Darmstadt, Germany) was set up to obtain a final concentration of 10 and 50 nmol/L in the transfection media as suggested by the manufacturer. Transfection medium was replaced with EGM2 complete medium after 5 hours, and the effect of miR-155 mimic on endothelial function (cell viability, angiogenesis, gene expression, and protein levels) was assessed after 24 hours.

Anti-miR-155 Inhibition Experiments In Vitro

The effects of CSC (20 µg/mL) on endothelial function (cell viability, angiogenesis, and protein levels) were assessed after 48 hours of treatment in the presence or absence of anti-miR 155 LNA (miRcurry LNA microRNA inhibitor, Qiagen) used at a final 50 nmol/L concentration following the manufacturer's instructions. Briefly, HUVECs were transfected with anti-miR-155 LNA diluted in Opti-MEM reduced serum medium (OPTIMEM) with lipofectamine transfection agent (Lipofectamine RNAimax, Invitrogen, Carlsbad, CA) for 5 hours. Transfection medium was then replaced with EGM2 complete medium with or without CSC at the aforementioned concentration.

MTT Assay

Cell survival was evaluated using the MTT reagent (Sigma Aldrich–Merck, Darmstadt, Germany). Control and treated HUVECs were incubated for 5 hours with MTT, and the absorbance of the solubilized substrate was measured with a microplate reader (Biorad, Milan, Italy) at 570 nm.

Matrigel Assay

Angiogenesis was performed by Matrigel assay. Briefly, Matrigel matrix growth factor reduced (BD Biosciences) was seeded in a 35-mm culture dish and allowed to solidify for 1 hour at 37°C. HUVECs collected after each specific treatment (described previously) were seeded on top of the Matrigel layer and incubated for 24 hours. Images were taken with an optical microscope (Zeiss, Jena, Germany) fitted with a digital camera, and the number of branching points was quantified from 3 to 10 randomly chosen fields using ImageJ software (National Institutes of Health, Bethesda, MD).

Gene Expression Analyses

TNF-α (tumor necrosis factor α) and interleukin (*IL*)-6 gene expressions were assessed in HUVECs by quantitative reverse transcriptase–polymerase chain reaction analysis. Total RNA was extracted by Trizol (Invitrogen, Milan, Italy), purified with DNase and retrotranscribed into cDNA using SuperScript VIL0 Master Mix (Invitrogen). Quantitative reverse transcriptase–polymerase chain reaction analysis was performed using the ViiA7 Real-Time PCR System and SYBR Select Master Mix 2X (Applied Biosystem, Foster City, CA). miR-155 precursor gene (*Pri-miR-155*) (*hBIC*) expression was assessed by quantitative reverse transcriptase–polymerase chain reaction analysis using validated primers²⁵ for the amplification of the unprocessed transcript encoding for miR-155. The amount of cDNA target was normalized using *GAPDH* (glyceraldehyde 3-phosphate dehydrogenase) as housekeeping gene and calculated by the comparative 2^{−ΔΔCt} method.²⁰ Used primers were as follows: *TNF-α* sense: CATCTTCTCGAACCCCGAGT; *TNF-α* antisense: CACCAGCTGGTTATCTCTCA; *IL-6* sense: GCTGCAGGCACAGAACCA; *IL-6* antisense: GC TGCGCAGAATGAGATGAG; *hBIC* sense: ACCAGAGAC CTTACCTGTACCTT; *hBIC* antisense: GGCATAAAG AATTTAAACACAGATTT; *GAPDH* sense: CAAGGCT GTGGGCAAGGT; *GAPDH* antisense: GGAAGGCCAT GCCAGTGA.

Western Blot Analysis

Samples were lysed in radioimmunoprecipitation assay buffer, separated by SDS-PAGE and transferred

onto polyvinylidene difluoride membranes (Amersham, Piscataway, NJ). Membranes were blocked in 5% non-fat dried milk (Biorad) and incubated overnight with the following primary antibodies: vascular endothelial growth factor (VEGF) (Abcam, Cambridge, UK), endothelial NO synthetase (Cell Signaling Technology, Danvers, MA), GAPDH (Santa Cruz Biotechnology, Santa Cruz, CA), and β -Actin (Santa Cruz). Detection was performed using ECL prime (Amersham Biosciences, CA).

H₂O₂ and NO Detection

H₂O₂ production and NO metabolites nitrite and nitrate were detected in HUVECs conditioned media by commercially available kits (Arbor Assay, Ann Arbor, MI). Experiments were performed following the manufacturer's protocol and values were expressed in μ mol/L.

Animal Studies

Vascular reactivity experiments were performed on mesenteric arteries isolated from 8-week-old male wild-type mice (C57BL6/J, N=6). Vessels were placed in a pressure myograph system filled with Krebs solution and transfected for 6 hours with 50 nmol/L of a mouse-specific anti-miR-155 LNA (miRcury LNA microRNA inhibitor, Qiagen) in the presence of the transfection reagent (Lipofectamine RNAimax, Invitrogen, Carlsbad, CA). Control vessels were incubated with a mouse-specific anti-miR negative control (miRCURY LNA microRNA Inhibitor Control, Qiagen). Vasorelaxation was assessed by measuring the dilatory responses of mesenteric arteries to cumulative concentrations of acetylcholine (from 10⁻⁹ to 10⁻⁵ mol/L) in vessels precontracted with phenylephrine as previously reported.²⁶ Responses were assessed after incubation with or without CSC treatment (1 μ g/mL) for 1 hour. Oxidative stress levels in vessels was assessed by dihydroethidium staining (Sigma Aldrich) as previously described.²⁷ Fluorescence intensity was quantified by ImageJ software. All studies involving animals were performed in accordance with the Italian and European Community (Directive 2010/63/EU) for animal experiments, and the protocol was approved by Sapienza University Animal Care Review Board. Mice were euthanized by cervical dislocation, and vessels were isolated for vascular reactivity experiments.

Statistical Analysis

Results are reported as mean \pm SEM of independent experiments. In vitro experiments were performed at least 3 times, and nonparametric tests were used for comparisons because of the small

number of independent replicates in different groups. Comparisons between 2 groups were performed by Mann–Whitney nonparametric tests. Statistical analysis between multiple groups was performed by Kruskal–Wallis nonparametric test followed by Conover post hoc analysis.

For human subject analyses, microRNA serum level significance was assessed by the Wilcoxon signed-rank test (matched pairs) for non-normalized values. On the other hand, 1-sample Student *t* tests were performed for miR-155-fold change in serum samples after checking for normal distribution of the values.

In ex vivo mouse experiments, 2-way analysis of variance followed by the Tukey multiple comparisons test was used for vascular reactivity assessment.

Graph Pad Prism software (GraphPad Software, Inc. La Jolla, CA), (MedCalc statistical software, MedCalc Software Ltd, Ostend, Belgium), and the R statistic package (R Foundation for Statistical Computing, Vienna, Austria) were used for the statistical analyses, and statistical significance was set at the 2-tailed 0.05 level.

RESULTS

We quantified the expression levels of several endothelial-related microRNAs based on the available literature^{8,9,28,29} (listed in Figure 1A and Table S1) in sera obtained from 40 healthy subjects before and after smoking 1 tobacco cigarette. Raw data analysis was performed on the linearized cycle threshold (Ct) value (2^{-Ct}) to assess the overall detection level of each miRNA. Some microRNAs were not detectable and were therefore excluded from further analysis (Figure 1A). We compared the detection level of each microRNA in each subject and found that miR-155 was the only microRNA to be significantly affected by smoking, with a significant increase of its circulating levels after a cigarette consumption (Figure 1A and 1B). Normalized expression levels also confirmed this result, showing a 1.8-fold increase of circulating miR-155 levels in the study subjects after smoking 1 cigarette (Figure 1C).

To test whether endothelial cells may represent a possible origin of circulating miR-155 after cigarette smoking, we tested whether CSC could induce miR-155 release in cultured endothelial cells. We therefore used HUVECs treated with CSC to mimic smoking stress in vitro and measured the intracellular and extracellular levels of miR-155 after 30 minutes, 1 hour, 4 hours, and 12 hours of treatment. We found that miR-155 levels significantly increased in culture medium of cells treated with CSC over time with respect to control cells (Figure 2A), without evidence of increased

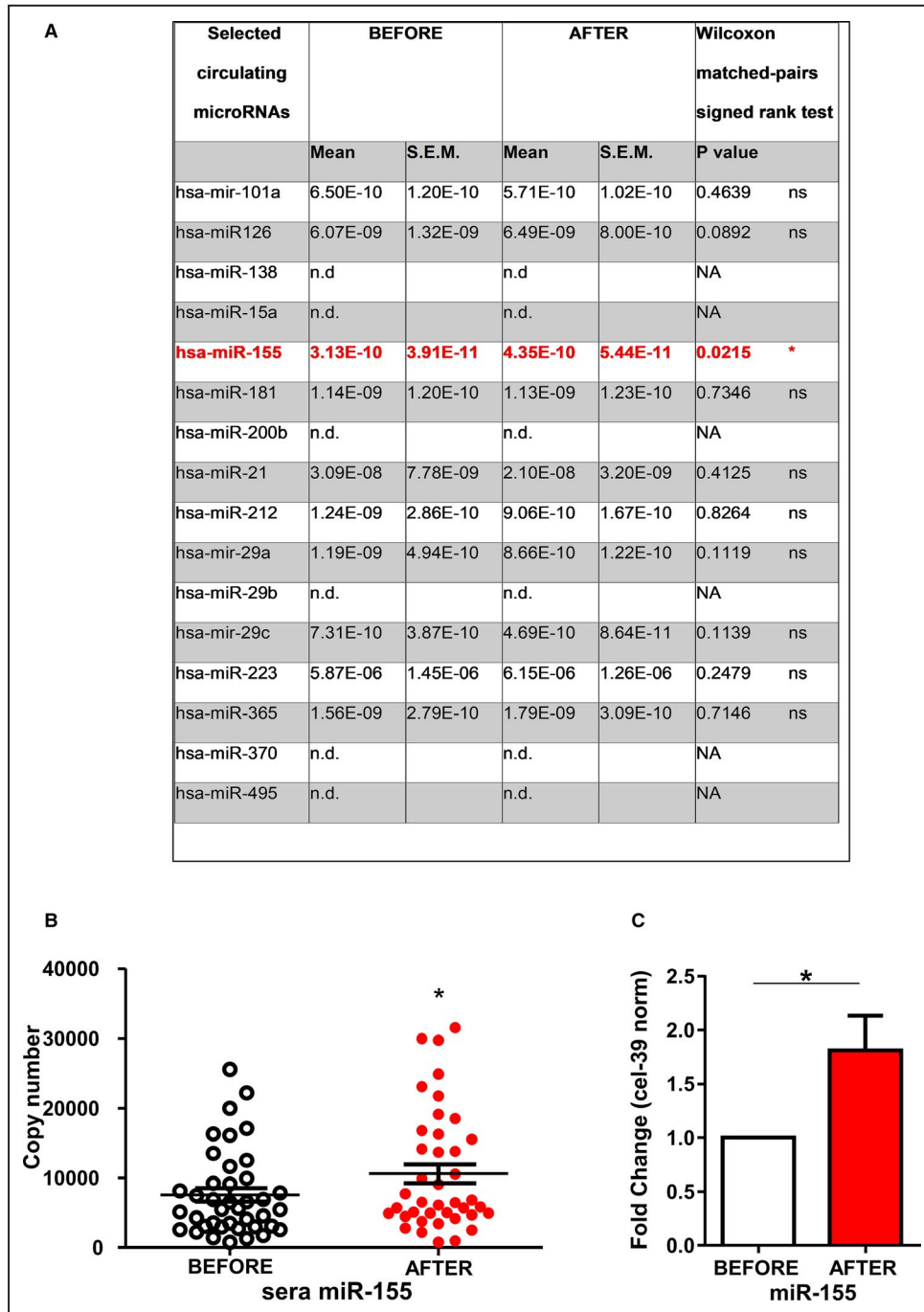


Figure 1. Cigarette smoke increases circulating miR-155 levels in healthy subjects. **A**, Table listing the assessed microRNAs levels in sera before and after cigarette smoking. **B**, Dot plot showing quantitative polymerase chain reaction quantification of miR-155 relative copy number in paired samples from 40 individuals before and after smoking 1 cigarette. Mean±SEM (N=40); *P<0.05, obtained using the Wilcoxon signed-rank test, matched pairs for non-normalized values. **C**, Bar graph showing cel-39 normalized miR-155 relative average fold change after smoking 1 cigarette (after) with respect to baseline levels (before) in the study population. Mean±SEM (N=40). *P<0.05, obtained using the Student *t* test. NA indicates not applicable; n.d., not detectable; and ns, not significant.

cellular damage or membrane disruption up to 4 hours (Figure 2D). On the other hand, FACS analysis revealed an increased apoptosis after 12 hours in CSC-treated

cells, suggesting that miR-155 extracellular accumulation may also be attributable to membrane alterations or cell disruption after prolonged CSC treatment

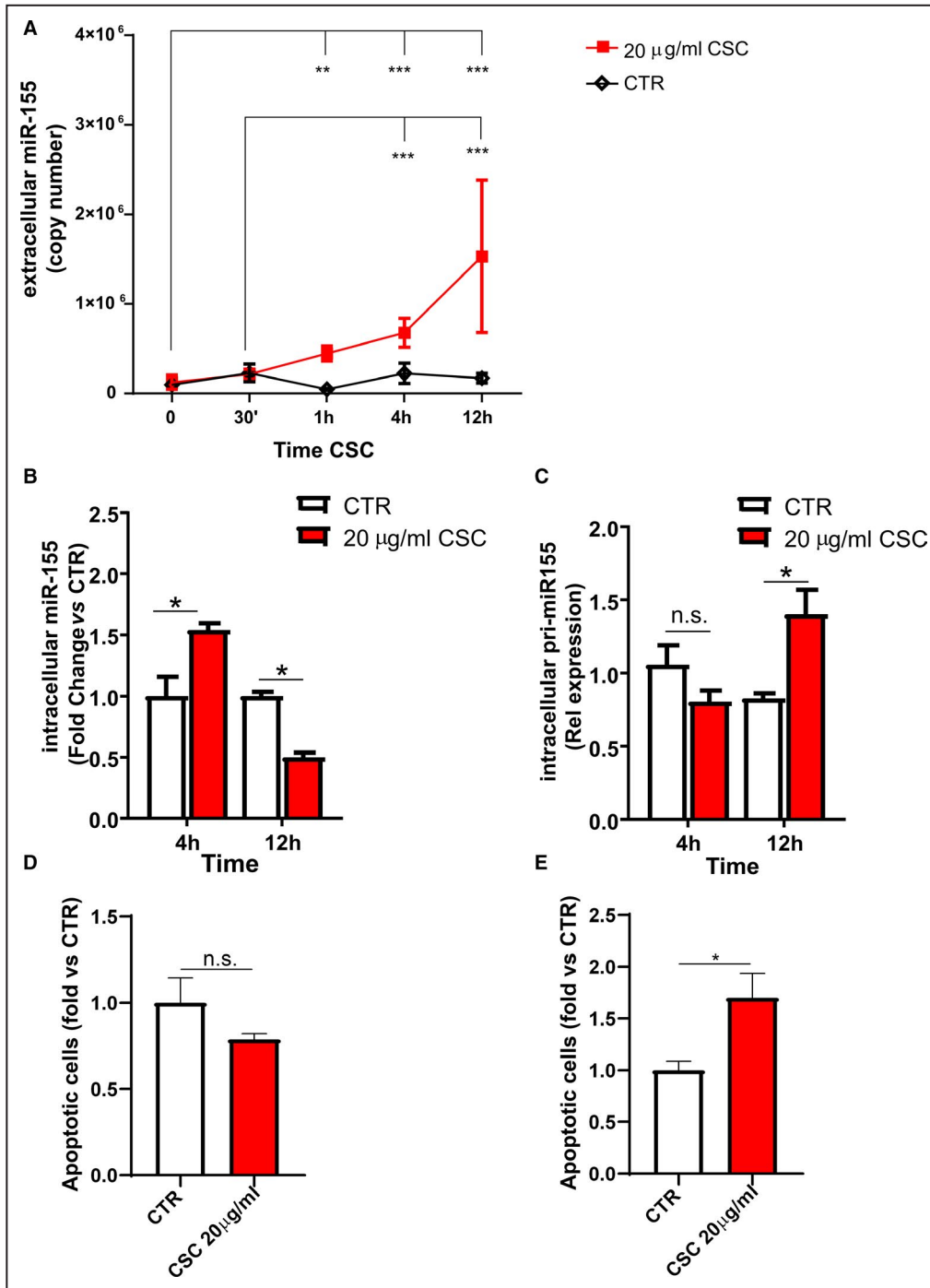


Figure 2. Cigarette smoke condensate (CSC) increases miR-155 in human umbilical vein endothelial cells.

A, Graph showing quantification of extracellular miR-155 (copy number) in cell culture supernatants collected from cigarette smoke condensate (CSC)-treated cells (red line) and DMSO-treated (control [CTR]) cultures (black line) at the indicated time points. CSC was used at 20 µg/ml concentration. ** $P < 0.01$ and *** $P < 0.001$ obtained by Kruskal–Wallis nonparametric test followed by Conover post hoc analysis. **B** and **C**, Bar graphs showing the intracellular miR-155 (**B**) and pri-miR-155 (**C**) relative expression measured in DMSO (CTR) and CSC-treated human umbilical vein endothelial cells at 4 and 12 hours. Gene expression was normalized to either U6 small nuclear RNA (snoRNA) or *GAPDH* for miR and pri-miR, respectively. * $P < 0.05$ obtained by Kruskal–Wallis nonparametric test followed by Conover post hoc analysis. **D** and **E**, Bar graph showing the percentage of apoptotic human umbilical vein endothelial cells (Annexin V positive) at 4 (**D**) and 12 hours (**E**) in DMSO control (CTR) and CSC-treated cells. * $P < 0.05$ obtained by Mann–Whitney nonparametric test. All data are presented as mean ± SEM (N=3–4). n.s. indicates not significant.

(Figure 2E). For this reason, we did not evaluate miR-155 accumulation at longer time points. We also observed an increase in intracellular miR-155 levels after 4 hours of treatment compared with untreated cells (Figure 2B). In contrast, we did not see an intracellular increase of miR-155 precursor gene (pri-miR-155) at the same time point (Figure 2C). Conversely, intracellular miR-155 levels decreased after 12 hours of CSC treatment, suggesting that miR-155 is continuously synthesized, released, and probably up-taken by endothelial cells in response to CSC treatment (Figure 2B and 2C).

Because smoking stress induces reactive oxygen species generation in endothelial cells, we assessed whether oxidative stress is sufficient to promote the extrusion of miR-155 by endothelial cells. Therefore, we treated HUVECs with 100 $\mu\text{mol/L}$ H_2O_2 and observed an increase in miR-155 accumulation in culture media of treated cells, in line with the results obtained with CSC treatment (Figure 3A and 3B).

We then tested whether miR-155 may contribute to the detrimental endothelial effects of smoking. For this purpose, we treated endothelial cells with CSC in the presence or absence of a specific inhibitor of miR-155. As expected, we found that CSC impaired angiogenesis (Figure 4A and 4B) and cell survival (Figure 4C) and drastically increased H_2O_2 (Figure 4D). Notably, these effects were attenuated by anti-miR-155 treatment (Figure 4A through 4D). Similarly, we also found a significant reduction of endothelial NO synthetase expression levels (Figure 4E, Figure S1) and NO production

(Figure 4F) in response to CSC treatment, which were rescued by anti-miR-155 (Figure 4E and 4F, Figure S1).

We also observed that miR-155 inhibition blunted CSC-induced reduction of vasorelaxation in response to acetylcholine in isolated vessels from mice (Figure 5A) along with a significant reduction of oxidative stress (Figure 5B and 5C).

These data suggest that miR-155 plays a role in mediating the deleterious effects of smoking stress in endothelial function both in vitro and ex vivo.

Finally, to further explore the biological significance of miR-155 accumulation by smoking stress, we evaluated the effects of its overexpression in endothelial cells by using a synthetic miR-155 mimic. We found that exogenous administration of miR-155 decreased cell viability (Figure 6A). In addition, miR-155 strongly impaired capillary network formation and reduced the number of branch points compared with untreated cells, indicating a reduced angiogenesis (Figure 6B and 6C). miR-155 mimic administration was also associated with increased gene expression of *IL-6* and *TNF- α* (Figure 6D). Finally, we found that miR-155 administration strongly reduced protein levels of VEGF and endothelial NO synthetase (Figure 6E and 6F; Figure S2A and S2B).

DISCUSSION

In our study, we demonstrated that smoking 1 single cigarette is sufficient to induce a rapid release of miR-155

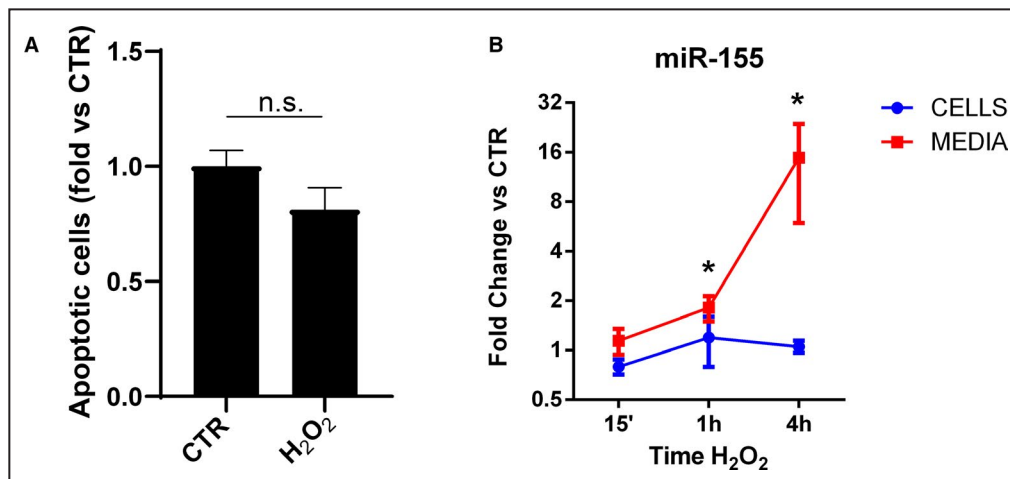


Figure 3. Oxidative stress increases extracellular miR-155 accumulation in human umbilical vein endothelial cells.

A, Bar graph showing the percentage of apoptosis in untreated control cells (CTR) and after 4 hours of treatment with 100 $\mu\text{mol/L}$ H_2O_2 (H_2O_2). Mann–Whitney nonparametric test. **B**, Time course measurement of miR-155 levels during H_2O_2 treatment in cell lysates (blue line) and conditioned media (red line) showing fold change with respect to untreated cells at each time point. * $P < 0.05$ compared to untreated cells (CTR) obtained by Kruskal–Wallis nonparametric test followed by Conover post hoc analysis. All data are presented as mean \pm SEM (N=3–4). n.s. indicates not significant.

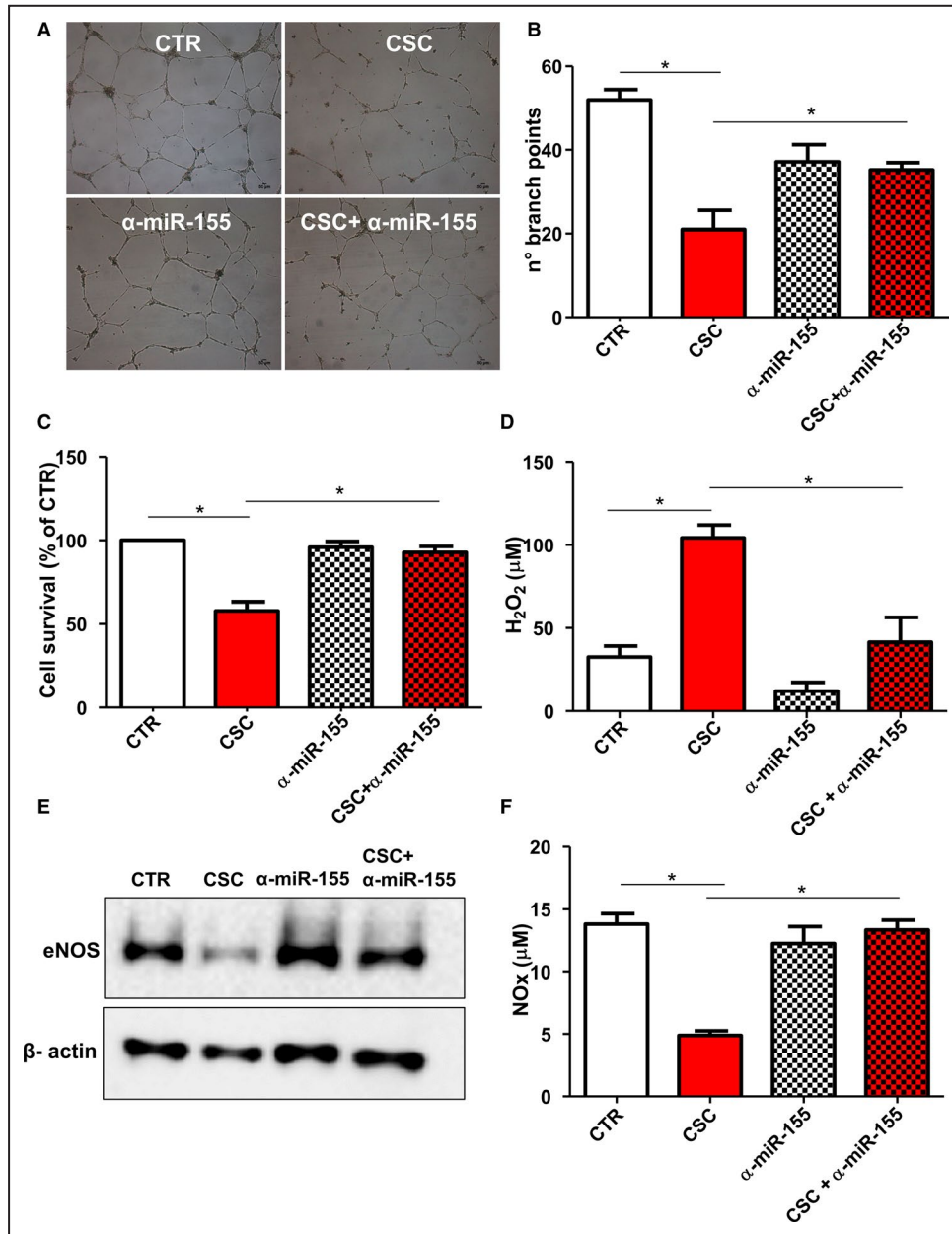


Figure 4. Anti-miR-155 blunts the deleterious effects of CSC on angiogenesis, cell survival, H₂O₂, and NO metabolism in endothelial cells.

A and B, Representative images of human umbilical vein endothelial cells angiogenesis assessed by Matrigel assay (scale bar=50 μm) (**A**) and bar graph showing relative quantification of branch point number (**B**) (N=3). **C,** Bar graph showing the percentage of human umbilical vein endothelial cells viability in each condition measured by MTT assay. Viability of CTR was set as 100% (N=3). **D,** Bar graph showing H₂O₂ concentration in cell supernatants collected in each condition (N=3). **E,** Representative image of Western blot analysis of eNOS expression (1 of 3 similar experiments). **F,** NOx levels in cell supernatants (N=3–9). Cells were treated for 48 hours with 20 μg/mL CSC either in the presence or absence of 50 nmol/L anti-miR 155 (α-miR-155). **P*<0.05 obtained by using nonparametric Kruskal-Wallis test followed by Conover post hoc analysis. All data are presented as mean±SEM. CSC indicates cigarette smoke condensate; CTR, DMSO-treated control cells; eNOS, endothelial NO synthetase; and NOx, NO metabolite.

in the bloodstream of healthy individuals. We also observed that smoke stress promotes the release of miR-155 from endothelial cells. However, miR-155 extracellular

accumulation after 12 hours may also be attributable to cellular damage because we observed increased apoptosis after 12 hours of CSC exposure. miR-155 inhibition

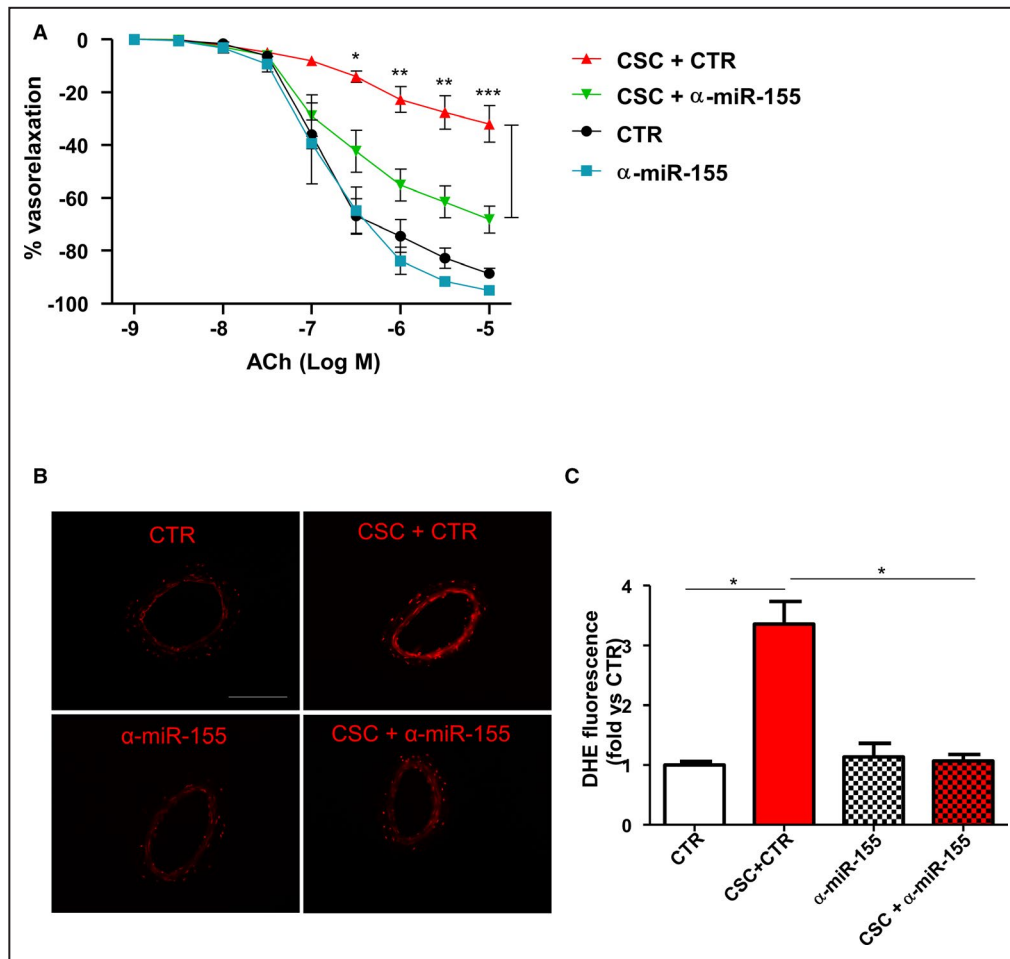


Figure 5. Anti-miR-155 blunts the deleterious effects of CSC on endothelial relaxation and oxidative stress of mouse mesenteric arteries.

A, Mesenteric arteries from wild-type C57BL6/J mice were transfected ex vivo with 50 nmol/L anti-miR-155 (α -miR-155) and incubated with 1 μ g/mL cigarette smoke condensate (CSC) for 1 hour. Control vessels were incubated with 50 nmol/L anti-miR negative control (CTR) and treated with CSC. Light blue and black α -miR-155 and CTR lines, respectively, represent vessels without CSC treatment. * P <0.05, ** P <0.01, and *** P <0.001 obtained by using 2-way analysis of variance followed by Tukey's multiple comparison test. **B** and **C**, Representative images of dihydroethidium (DHE) staining and relative quantification (scale bar=100 μ m). * P < 0.05 obtained by nonparametric Kruskal-Wallis test followed by Conover post hoc analysis. All data are presented as mean \pm SEM (N=6).

could rescue angiogenesis, cell survival, NO metabolism, and redox status in endothelial cells treated with CSC. It also restored vascular function and oxidative stress in isolated arteries exposed to smoke stress. miR-155 mimic administration was also sufficient to mimic the effects of smoke stress. We also found that reactive oxygen species induced miR-155 release by endothelial cells, whereas miR-155 inhibition blunted oxidative stress both in vitro and ex vivo, suggesting a detrimental synergistic feedback loop between miR-155 and oxidative stress.

Our data extend previous evidence demonstrating the involvement of miR-155 in vascular pathophysiology. Previous studies showed that inflammation and oxidative stress increase endothelial miR-155 expression, leading to endothelial dysfunction.^{30,31} Inhibition

of miR-155 ameliorates endothelium-dependent relaxation.³⁰ Remarkably, endothelial NO synthetase was shown to be a direct target of miR-155,³⁰ whereas VEGF levels were inversely correlated with miR-155 expression.³²

Data obtained in preclinical and clinical studies reported a close association between miR-155 plasma level and the development of cardiovascular diseases.^{33,34} For example, circulating miR-155 was suggested to have a prognostic value in patients with myocardial infarction and heart failure.³⁵⁻³⁸

Previous works attempted to address the impact of cigarette smoking on circulating microRNAs.³⁹⁻⁴¹ These studies demonstrated that smoking exposure induces a significant dysregulation in microRNAs

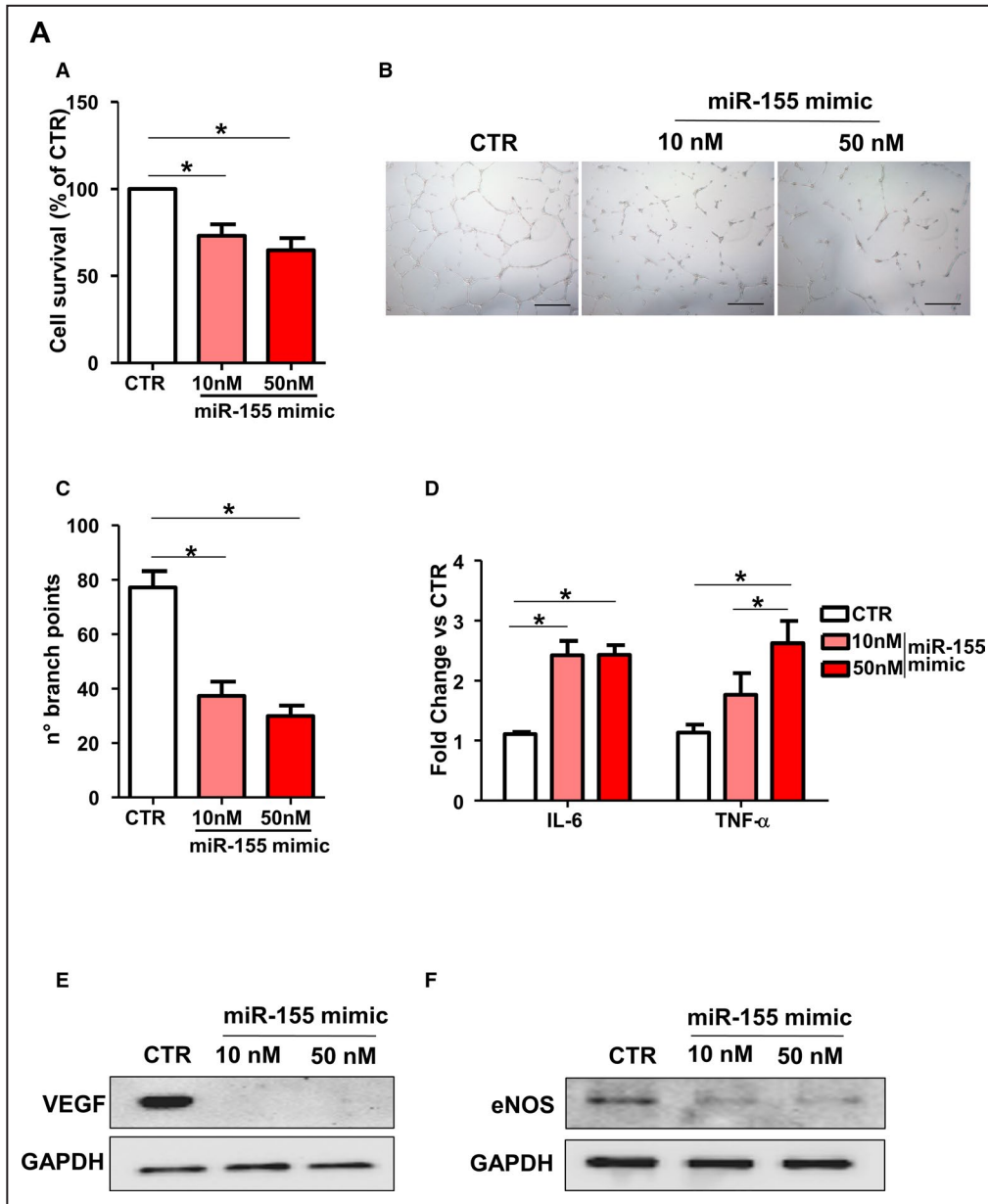


Figure 6. Exogenous miR-155 overexpression impairs cell survival, angiogenesis, inflammation and endothelial marker expression in human umbilical vein endothelial cells.

A, Bar graph showing the percentage of viable human umbilical vein endothelial cells treated with miR-155 mimic for 24 hours. **B**, Representative images of human umbilical vein endothelial cell angiogenesis assessed by Matrigel assay after exposure to different concentrations of miR-155 mimic (10 nmol/L, 50 nmol/L); scale bar=100 μm. **C**, Bar graph showing angiogenesis quantification as branchpoint count in each condition. **D**, Relative gene expression of IL-6 and TNF-α in human umbilical vein endothelial cells after miR-155 treatment for 24 hours. Fold change compared to CTR. **E** and **F**, Representative Western blot images of VEGF (**E**) and endothelial NO synthetase (eNOS) (**F**) in human umbilical vein endothelial cells transfected with miR-155 mimic. **P*<0.05 compared to untreated cells (CTR) obtained using the nonparametric Kruskal-Wallis test followed by Conover post hoc analysis. All data are presented as mean±SEM (N=3). CTR indicates nontransfected control cells; eNOS, endothelial NO synthetase; IL-6, interleukin-6; TNF-α, tumor necrosis factor α; and VEGF, vascular endothelial growth factor.

plasma profile either in smokers or in former smokers. However, in these studies it was impossible to understand whether the observed dysregulation of microRNAs was a direct consequence of smoke exposure or

whether it was rather the consequence of smoke-related pathologies. In our study, we demonstrated for the first time that smoking 1 cigarette is sufficient to induce a rapid release of miR-155 in the bloodstream

of healthy subjects free of any disease. Based on the observed detrimental effects of miR-155 in endothelial cells, we speculate that miR-155 increase after smoking each tobacco cigarette may represent an insult on endothelial cells, contributing in the long-term to the development of protracted inflammation and endothelial dysfunction. Future studies are warranted to test this hypothesis. However, this view is supported by our current results showing that the detrimental effects of smoking stress are attenuated by miR-155 inhibition.

It will also be interesting to test whether miR-155 could represent a valid biomarker for the risk stratification of subjects who smoke or for a proper evaluation of the safety profile of modified risk products, such as electronic cigarettes and heat-not-burn cigarettes.⁴²

Several limitations in our study should also be acknowledged. First, we did not conduct an unbiased large screening of circulating microRNA before and after tobacco smoking, whereas the choice of the studied microRNAs was based on the literature. In addition, we only tested the acute effects of tobacco smoking on miR-155 release in the bloodstream, and we did not evaluate whether this is chronically correlated with vascular damage in subjects who smoke. The effects of chronic cigarette smoking or different nicotine contents on microRNAs expression need to be elucidated in future studies. Finally, when we analyzed the effects of acute smoking on circulating microRNA levels in our human samples, we did not correct for multiple testing because of the small sample size. However, we believe that our in vitro and ex vivo biological experiments substantiated the human results, fully confirming the involvement of miR-155 in the development of smoking-induced endothelial damage.

In conclusion, our data suggest that miR-155 is involved in the development of endothelial damage induced by smoking stress.

ARTICLE INFORMATION

Received July 17, 2020; accepted October 27, 2020.

Affiliations

From the Department of Medical-Surgical Sciences and Biotechnologies, Sapienza University of Rome, Latina, Italy (G.F., A.B., I.C., V.P., E.C., R.C., S.S., D.V., E.D.F., G.B.-Z., F.P., S.S.); IRCCS Neuromed, Pozzilli, Italy (G.F., M.F., F.d.N., R.S., F.B., S.M., S.R., M.V., S.S.); Mediterranean Cardiocentro-Napoli, Napoli, Italy (I.C., R.C., E.D.F., G.B.-Z.); Department of Internal Medicine and Medical Specialties (C.N.) and Department of Clinical and Molecular Medicine, School of Medicine and Psychology (S.R., M.V.), Sapienza University of Rome, Rome, Italy; Center for Molecular Cardiology, University of Zürich, Switzerland (F.P.); Cardiology, University Heart Center, University Hospital Zurich, Zurich, Switzerland (F.P.); and Department of Cardiology, Ospedale Santa Maria Goretti, Latina, Italy (F.V.).

Sources of Funding

This work was supported by a grant from the Italian Ministry of Health to G.F., M.V., S.R., S.S.; by a grant from the Italian Ministry of Health (PRIN_2017N8K7S2_002); by the "5 per mille" grant to S.R. and M.V.; by the Sapienza University-Avvio alla Ricerca grant to F.P. (protocol AR21816427B07019); and from the Pasteur Institute, Cenci-Bolognietti Foundation to S.S.

Disclosures

None.

Supplementary Material

Table S1

Figures S1–S2

References 43–72

REFERENCES

- Cardiovascular disease in Europe: an epidemiological update. *Eur Heart J*. 2016;37:3182-3183.
- Messner B, Bernhard D. Smoking and cardiovascular disease: mechanisms of endothelial dysfunction and early atherogenesis. *Arterioscler Thromb Vasc Biol*. 2014;34:509-515.
- Aune D, Schlesinger S, Norat T, Riboli E. Tobacco smoking and the risk of sudden cardiac death: a systematic review and meta-analysis of prospective studies. *Eur J Epidemiol*. 2018;33:509-521.
- Primates P, Falaschetti E, Gupta S, Marmot MG, Poulter NR. Association between smoking and blood pressure: evidence from the health survey for England. *Hypertension*. 2001;37:187-193.
- Loffredo L, Carnevale R, Perri L, Catasca E, Augelletti T, Cangemi R, Albanese F, Piccheri C, Nocella C, Pignatelli P, et al. NOX2-mediated arterial dysfunction in smokers: acute effect of dark chocolate. *Heart*. 2011;97:1776-1781.
- Carnevale R, Sciarretta S, Violi F, Nocella C, Loffredo L, Perri L, Peruzzi M, Marullo AG, De Falco E, Chimenti I, et al. Acute impact of tobacco vs electronic cigarette smoking on oxidative stress and vascular function. *Chest*. 2016;150:606-612.
- Mendell JT, Olson EN. MicroRNAs in stress signaling and human disease. *Cell*. 2012;148:1172-1187.
- Condorelli G, Latronico MV, Cavarretta E. MicroRNAs in cardiovascular diseases: current knowledge and the road ahead. *J Am Coll Cardiol*. 2014;63:2177-2187.
- Viereck J, Thum T. Circulating noncoding RNAs as biomarkers of cardiovascular disease and injury. *Circ Res*. 2017;120:381-399.
- Cavarretta E, Condorelli G. miR-21 and cardiac fibrosis: another brick in the wall? *Eur Heart J*. 2015;36:2139-2141.
- Stanzione R, Bianchi F, Cotugno M, Marchitti S, Forte M, Busceti C, Ryskalin L, Fornai F, Volpe M, Rubattu S. A decrease of brain microRNA-122 level is an early marker of cerebrovascular disease in the stroke-prone spontaneously hypertensive rat. *Oxid Med Cell Longev*. 2017;2017:1206420.
- Cheng Y, Tan N, Yang J, Liu X, Cao X, He P, Dong X, Qin S, Zhang C. A translational study of circulating cell-free microRNA-1 in acute myocardial infarction. *Clin Sci*. 2010;119:87-95.
- Peng L, Chun-guang Q, Bei-fang L, Xue-zhi D, Zi-hao W, Yun-fu L, Yan-ping D, Yang-gui L, Wei-guo L, Tian-yong H, et al. Clinical impact of circulating miR-133, miR-1291 and miR-663b in plasma of patients with acute myocardial infarction. *Diagn pathol*. 2014;9:89.
- He F, Lv P, Zhao X, Wang X, Ma X, Meng W, Meng X, Dong S. Predictive value of circulating miR-328 and miR-134 for acute myocardial infarction. *Mol Cell Biochem*. 2014;394:137-144.
- Cavarretta E, Frati G. MicroRNAs in coronary heart disease: ready to enter the clinical arena? *Biomed Res Int*. 2016;2016:2150763.
- Guay C, Regazzi R. Circulating microRNAs as novel biomarkers for diabetes mellitus. *Nat Rev Endocrinol*. 2013;9:513-521.
- Romaine SP, Charchar FJ, Samani NJ, Tomaszewski M. Circulating microRNAs and hypertension—from new insights into blood pressure regulation to biomarkers of cardiovascular risk. *Curr Opin Pharmacol*. 2016;27:1-7.
- Thum T, Condorelli G. Long noncoding RNAs and microRNAs in cardiovascular pathophysiology. *Circ Res*. 2015;116:751-762.
- Chimenti I, Pagano F, Cavarretta E, Angelini F, Peruzzi M, Barretta A, Greco E, De Falco E, Marullo AG, Sciarretta S, et al. Beta-blockers treatment of cardiac surgery patients enhances isolation and improves phenotype of cardiosphere-derived cells. *Sci Rep*. 2016;6:36774.
- Livak KJ, Schmittgen TD. Analysis of relative gene expression data using real-time quantitative pcr and the 2(-delta delta c(t)) method. *Methods*. 2001;25:402-408.
- Kalra VK, Ying Y, Deemer K, Natarajan R, Nadler JL, Coates TD. Mechanism of cigarette smoke condensate induced adhesion of human monocytes to cultured endothelial cells. *J Cell Physiol*. 1994;160:154-162.

22. Snajdar RM, Busuttill SJ, Averbook A, Graham DJ. Inhibition of endothelial cell migration by cigarette smoke condensate. *J Surg Res*. 2001;96:10-16.
23. Kayyali US, Budhiraja R, Pennella CM, Cooray S, Lanzillo JJ, Chalkley R, Hassoun PM. Upregulation of xanthine oxidase by tobacco smoke condensate in pulmonary endothelial cells. *Toxicol Appl Pharmacol*. 2003;188:59-68.
24. Chimenti I, Pagano F, Angelini F, Siciliano C, Mangino G, Picchio V, De Falco E, Peruzzi M, Carnevale R, Ibrahim M, et al. Human lung spheroids as in vitro niches of lung progenitor cells with distinctive paracrine and plasticity properties. *Stem Cells Transl Med*. 2017;6:767-777.
25. Wood CD, Carvell T, Gunnell A, Ojienyi OO, Osborne C, West MJ. Enhancer control of microRNA miR-155 expression in Epstein-Barr virus-infected B cells. *J Virol*. 2018;92.
26. Villa F, Carrizzo A, Spinelli CC, Ferrario A, Malovini A, Maciag A, Damato A, Auricchio A, Spinetti G, Sangalli E, et al. Genetic analysis reveals a longevity-associated protein modulating endothelial function and angiogenesis. *Circ Res*. 2015;117:333-345.
27. Schiattarella GG, Carrizzo A, Iardi F, Damato A, Ambrosio M, Madonna M, Trimarco V, Marino M, De Angelis E, Settembrini S, et al. Rac1 modulates endothelial function and platelet aggregation in diabetes mellitus. *J Am Heart Assoc*. 2018;7.
28. Schulte C, Karakas M, Zeller T. MicroRNAs in cardiovascular disease – clinical application. *Clin Chem Lab Med*. 2017;55:687-704.
29. Neth P, Nazari-Jahanfogh M, Schober A, Weber C. MicroRNAs in flow-dependent vascular remodeling. *Cardiovasc Res*. 2013;99:294-303.
30. Sun HX, Zeng DY, Li RT, Pang RP, Yang H, Hu YL, Zhang Q, Jiang Y, Huang LY, Tang YB, et al. Essential role of microRNA-155 in regulating endothelium-dependent vasorelaxation by targeting endothelial nitric oxide synthase. *Hypertension*. 2012;60:1407-1414.
31. Liu Y, Pan Q, Zhao Y, He C, Bi K, Chen Y, Zhao B, Chen Y, Ma X. MicroRNA-155 regulates ROS production, no generation, apoptosis and multiple functions of human brain microvessel endothelial cells under physiological and pathological conditions. *J Cell Biochem*. 2015;116:2870-2881.
32. Liu Q, Yang J. Expression and significance of miR155 and vascular endothelial growth factor in placenta of rats with preeclampsia. *Int J Clin Exp Med*. 2015;8:15731-15737.
33. Cao RY, Li Q, Miao Y, Zhang Y, Yuan W, Fan L, Liu G, Mi Q, Yang J. The emerging role of microRNA-155 in cardiovascular diseases. *Biomed Res Int*. 2016;2016:9869208.
34. Welten SM, Goossens EA, Quax PH, Nossent AY. The multifactorial nature of microRNAs in vascular remodeling. *Cardiovasc Res*. 2016;110:6-22.
35. Matsumoto S, Sakata Y, Nakatani D, Suna S, Mizuno H, Shimizu M, Usami M, Sasaki T, Sato H, Kawahara Y, et al. A subset of circulating microRNAs are predictive for cardiac death after discharge for acute myocardial infarction. *Biochem Biophys Res Commun*. 2012;427:280-284.
36. Xie W, Li P, Wang Z, Chen J, Lin Z, Liang X, Mo Y. Rosuvastatin may reduce the incidence of cardiovascular events in patients with acute coronary syndromes receiving percutaneous coronary intervention by suppressing miR-155/SHIP-1 signaling pathway. *Cardiovasc Ther*. 2014;32:276-282.
37. Ikitimur B, Cakmak HA, Coskunpinar E, Barman HA, Vural VA. The relationship between circulating microRNAs and left ventricular mass in symptomatic heart failure patients with systolic dysfunction. *Kardiologia polska*. 2015;73:740-746.
38. Marques FZ, Vizi D, Khammy O, Mariani JA, Kaye DM. The transcardiac gradient of cardio-microRNAs in the failing heart. *Eur J Heart Fail*. 2016;18:1000-1008.
39. Banerjee A, Waters D, Camacho OM, Minet E. Quantification of plasma microRNAs in a group of healthy smokers, ex-smokers and non-smokers and correlation to biomarkers of tobacco exposure. *Biomarkers*. 2015;20:123-131.
40. Takahashi K, Yokota S, Tsumi N, Fukami T, Yokoi T, Nakajima M. Cigarette smoking substantially alters plasma microRNA profiles in healthy subjects. *Toxicol Appl Pharmacol*. 2013;272:154-160.
41. Shi B, Gao H, Zhang T, Cui Q. Analysis of plasma microRNA expression profiles revealed different cancer susceptibility in healthy young adult smokers and middle-aged smokers. *Oncotarget*. 2016;7:21676-21685.
42. Biondi-Zoccai G, Sciarretta S, Bullen C, Nocella C, Violi F, Loffredo L, Pignatelli P, Perri L, Peruzzi M, Marullo AGM, et al. Acute effects of heat-not-burn, electronic vaping, and traditional tobacco combustion cigarettes: the sapientia university of Rome-vascular assessment of proatherosclerotic effects of smoking (sur - vapes) 2 randomized trial. *J Am Heart Assoc*. 2019;8:e010455. 10.1161/JAHA.118.010455.
43. Chen K, Fan W, Wang X, Ke X, Wu G, Hu C. MicroRNA-101 mediates the suppressive effect of laminar shear stress on mTOR expression in vascular endothelial cells. *Biochem Biophys Res Commun*. 2012;427:138-142.
44. Kim JH, Lee KS, Lee DK, Kim J, Kwak SN, Ha KS, Choe J, Won MH, Cho BR, Jeoung D, et al. Hypoxia-responsive microRNA-101 promotes angiogenesis via heme oxygenase-1/vascular endothelial growth factor axis by targeting cullin 3. *Antioxid Redox Signal*. 2014;21:2469-2482.
45. Wang S, Aurora AB, Johnson BA, Qi X, McAnally J, Hill JA, Richardson JA, Bassel-Duby R, Olson EN. The endothelial-specific microRNA miR-126 governs vascular integrity and angiogenesis. *Dev Cell*. 2008;15:261-271.
46. Zampetaki A, Kiechl S, Drozdov I, Willeit P, Mayr U, Prokopi M, Mayr A, Weger S, Oberhollenzer F, Bonora E, et al. Plasma microRNA profiling reveals loss of endothelial miR-126 and other microRNAs in type 2 diabetes. *Circ Res*. 2010;107:810-817.
47. Li JB, Wang HY, Yao Y, Sun QF, Liu ZH, Liu SQ, Zhuang JL, Wang YP, Liu HY. Overexpression of microRNA-138 alleviates human coronary artery endothelial cell injury and inflammatory response by inhibiting the PI3k/Akt/eNOS pathway. *J Cell Mol Med*. 2017;21:1482-1491.
48. Sen A, Most P, Peppel K. Induction of microRNA-138 by pro-inflammatory cytokines causes endothelial cell dysfunction. *FEBS Lett*. 2014;588:906-914.
49. Yin KJ, Olsen K, Hamblin M, Zhang J, Schwendeman SP, Chen YE. Vascular endothelial cell-specific microRNA-15a inhibits angiogenesis in hindlimb ischemia. *J Biol Chem*. 2012;287:27055-27064.
50. Spinetti G, Fortunato O, Caporali A, Shantikumar S, Marchetti M, Meloni M, Descamps B, Floris I, Sangalli E, Vono R, et al. MicroRNA-15a and microRNA-16 impair human circulating proangiogenic cell functions and are increased in the proangiogenic cells and serum of patients with critical limb ischemia. *Circ Res*. 2013;112:335-346.
51. Lee KS, Kim J, Kwak SN, Lee KS, Lee DK, Ha KS, Won MH, Jeoung D, Lee H, Kwon YG, et al. Functional role of nf-kappab in expression of human endothelial nitric oxide synthase. *Biochem Biophys Res Commun*. 2014;448:101-107.
52. Kazenwadel J, Michael MZ, Harvey NL. Prox1 expression is negatively regulated by miR-181 in endothelial cells. *Blood*. 2010;116:2395-2401.
53. Sun X, Icli B, Wara AK, Belkin N, He S, Kobzik L, Hunninghake GM, Vera MP, Registry M, Blackwell TS, et al. MicroRNA-181b regulates nf-kappab-mediated vascular inflammation. *J Clin Invest*. 2012;122:1973-1990.
54. Magenta A, Cencioni C, Fasanaro P, Zaccagnini G, Greco S, Sarra-Ferraris G, Antonini A, Martelli F, Capogrossi MC. MiR-200c is upregulated by oxidative stress and induces endothelial cell apoptosis and senescence via zeb1 inhibition. *Cell Death Differ*. 2011;18:1628-1639.
55. Lo WY, Yang WK, Peng CT, Pai WY, Wang HJ. MicroRNA-200a/200b modulate high glucose-induced endothelial inflammation by targeting o-linked n-acetylglucosamine transferase expression. *Front Physiol*. 2018;9:355.
56. Weber M, Baker MB, Moore JP, Searles CD. MiR-21 is induced in endothelial cells by shear stress and modulates apoptosis and eNOS activity. *Biochem Biophys Res Commun*. 2010;393:643-648.
57. Sabatel C, Malvaux L, Bovy N, Deroanne C, Lambert V, Gonzalez ML, Colige A, Rakic JM, Noel A, Martial JA, et al. MicroRNA-21 exhibits antiangiogenic function by targeting RhoB expression in endothelial cells. *PLoS One*. 2011;6:e16979.
58. Kumarswamy R, Volkmann I, Beermann J, Napp LC, Jabs O, Bhayadia R, Melk A, Ucar A, Chowdhury K, Lorenzen JM, et al. Vascular importance of the miR-212/132 cluster. *Eur Heart J*. 2014;35:3224-3231.
59. Guarani V, DeFlorian G, Franco CA, Kruger M, Phng LK, Bentley K, Toussaint L, Dequiedt F, Mostoslavsky R, Schmidt MHH, et al. Acetylation-dependent regulation of endothelial notch signalling by the SIRT1 deacetylase. *Nature*. 2011;473:234-238.
60. Widlansky ME, Jensen DM, Wang J, Liu Y, Geurts AM, Krieger AJ, Liu P, Ying R, Zhang G, Casati M, et al. miR-29 contributes to normal endothelial function and can restore it in cardiometabolic disorders. *EMBO Mol Med*. 2018;10.
61. Corsten MF, Denert R, Jochems S, Kuznetsova T, Devaux Y, Hofstra L, Wagner DR, Staessen JA, Heymans S, Schroen B. Circulating microRNA-208b and microRNA-499 reflect myocardial damage in cardiovascular disease. *Circ Cardiovasc Genet*. 2010;3:499-506.
62. Boon RA, Seeger T, Heydt S, Fischer A, Hergenreider E, Horrevoets AJ, Vinciguerra M, Rosenthal N, Sciacca S, Pilato M, et al. MicroRNA-29 in aortic dilation: implications for aneurysm formation. *Circ Res*. 2011;109:1115-1119.

63. Shi L, Fisslthaler B, Zippel N, Fromel T, Hu J, Elgheznavy A, Heide H, Popp R, Fleming I. MicroRNA-223 antagonizes angiogenesis by targeting beta1 integrin and preventing growth factor signaling in endothelial cells. *Circ Res*. 2013;113:1320-1330.
64. Li S, Chen H, Ren J, Geng Q, Song J, Lee C, Cao C, Zhang J, Xu N. MicroRNA-223 inhibits tissue factor expression in vascular endothelial cells. *Atherosclerosis*. 2014;237:514-520.
65. Qin B, Xiao B, Liang D, Xia J, Li Y, Yang H. MicroRNAs expression in ox-LDL treated HUVECs: miR-365 modulates apoptosis and Bcl-2 expression. *Biochem Biophys Res Commun*. 2011;410:127-133.
66. Liu J, Zhu G, Xu S, Liu S, Lu Q, Tang Z. Analysis of miRNA expression profiling in human umbilical vein endothelial cells affected by heat stress. *Int J Mol Med*. 2017;40:1719-1730.
67. Qi L, Hongjuan H, Ning G, Zhengbin H, Yanjiang X, Tiebo Z, Zhijun H, Qiong W. miR-370 is stage-specifically expressed during mouse embryonic development and regulates Dnmt3a. *FEBS Lett*. 2013;587:775-781.
68. Zhang H, Sun X, Hao D. Upregulation of microRNA-370 facilitates the repair of amputated fingers through targeting forkhead box protein o1. *Exp Biol Med*. 2016;241:282-289.
69. Liu D, Zhang XL, Yan CH, Li Y, Tian XX, Zhu N, Rong JJ, Peng CF, Han YL. MicroRNA-495 regulates the proliferation and apoptosis of human umbilical vein endothelial cells by targeting chemokine CCL2. *Thromb Res*. 2015;135:146-154.
70. Zhou T, Xiang DK, Li SN, Yang LH, Gao LF, Feng C. MicroRNA-495 ameliorates cardiac microvascular endothelial cell injury and inflammatory reaction by suppressing the NLRP3 inflammasome signaling pathway. *Cell Physiol Biochem*. 2018;49:798-815.
71. Gidlof O, van der Brug M, Ohman J, Gilje P, Olde B, Wahlestedt C, Erlinge D. Platelets activated during myocardial infarction release functional mirna, which can be taken up by endothelial cells and regulate ICAM1 expression. *Blood*. 2013;121:S3901-3926.
72. Li J, Tan M, Xiang Q, Zhou Z, Yan H. Thrombin-activated platelet-derived exosomes regulate endothelial cell expression of ICAM-1 via microRNA-223 during the thrombosis-inflammation response. *Thromb Res*. 2017;154:96-105.

Supplemental Material

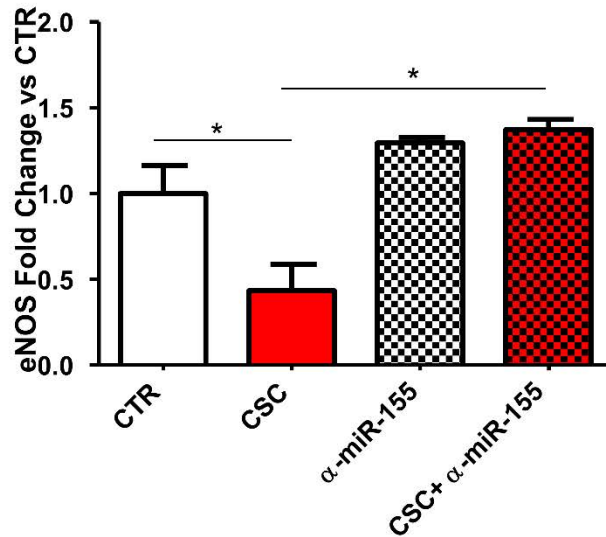
Table S1. Endothelial effects of miRNAs analyzed in our study population.

| Selected circulating microRNAs | Regulation | Target | References |
|---------------------------------------|---|--------------------------------------|-------------------|
| hsa-mir-101a | up-regulated in EC exposed to laminar shear stress | mTOR, Cullin 3 (HO-1/VEGF/eNOS axis) | 43,44 |
| hsa-miR126 | specifically expressed in the EC lineage and haematopoietic progenitor cells | PI3K/Akt/mTOR axis SPRED-1 | 45,46 |
| hsa-miR-138 | up-regulated in hypoxia-induced EC dysfunction | PI3K/Akt/eNOS | 47,48 |
| hsa-miR-15a | impairs tube formation, EC migration, and cell differentiation | FGF2, VEGF-A, AKT-3 | 49,50 |
| hsa-miR-155 | imbalanced in EC dysfunction | PI3K/Akt/eNOS NF-κB/eNOS | 30,51 |
| hsa-miR-181 | Inhibits downstream canonical NF-κB signaling pathway in EC | Prox1 Importin-α3 | 52,53 |
| hsa-miR-200b | modulates EC inflammation, up-regulated by oxidative stress | ICAM-1, VCAM-1, E-selectin ZEB1 | 54,55 |
| hsa-miR-21 | decrease EC migration via repression of RhoB and increased eNOS phosphorylation and NO production | PTEN RhoB eNOS | 56,57 |
| hsa-miR-212 | regulates EC migration and capillary tube formation on TGF-β stimulus | GAB1 SIRT1 | 58,59 |
| hsa-mir-29 | promotes EC-dependent vasodilation, NO | eNOS Matrix metalloproteinase | 60-62 |

| | | | |
|-------------|--|---|-------|
| | production and regulates EC differentiation | | |
| hsa-miR-223 | prevents EC angiogenic proliferation | Tissue Factor β 1 integrin | 63,64 |
| hsa-miR-365 | modulates EC inflammation and apoptosis | Bcl-2 | 65,66 |
| hsa-miR-370 | induces FoxO transcription factors, critical mediators of oxidative stress resistance | FOXO1 Dnmt3a | 67,68 |
| hsa-miR-495 | inhibits EC apoptosis and improves EC proliferation | CCL2 NLRP3, TNF- α , IL-1 β | 69,70 |
| cel-miR-39 | regulates the expression of adhesion molecules mainly by impacting NF- κ B and the MAPK pathway | ICAM1 | 71,72 |

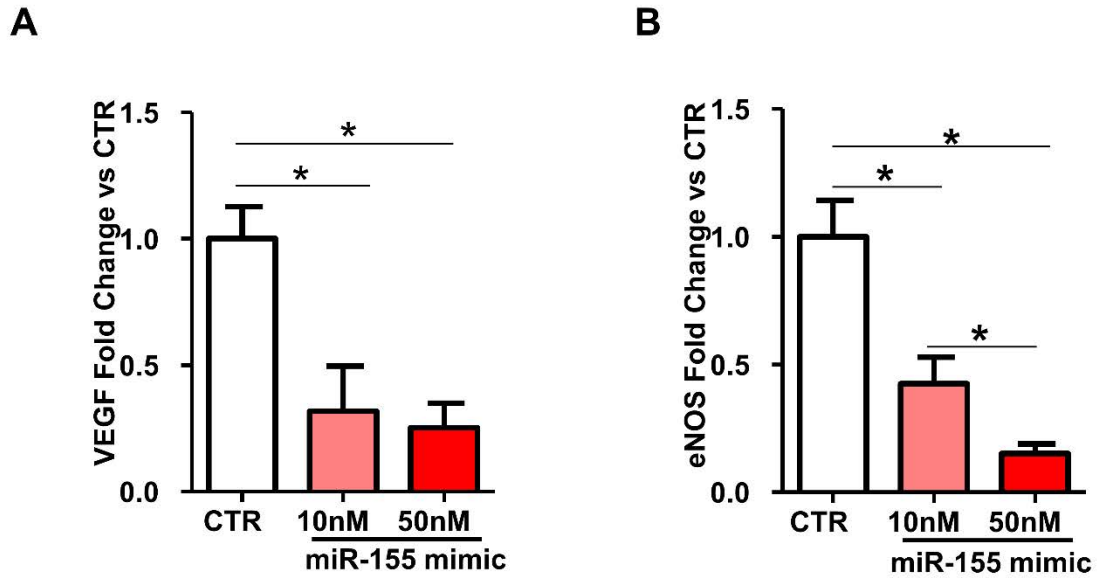
EC - endothelial cells; eNOS - nitric oxide synthase; NO - nitric oxide.

Figure S1. MiR-155 inhibition blunts the deleterious effects of CSC on eNOS expression.



Densitometric analysis of western blot for eNOS in HUVECs incubated with 20 $\mu\text{g}/\text{mL}$ CSC either in presence or absence of 50 nM anti-miR-155 (α -miR-155); CTR indicates untreated cells. * $p < 0.05$; obtained by using the non-parametric Kruskal-Wallis test followed by Conover's post-hoc analysis. All data are presented as mean \pm SEM (N=3).

Figure S2. miR-155 overexpression decreases VEGF and eNOS expression.



(A-B). Densitometric analyses of western blots for VEGF **(A)** and eNOS **(B)** in HUVECs treated with different concentrations of miR-155 mimic (10nM, 50nM). * $p < 0.05$ obtained by using the non-parametric Kruskal-Wallis test followed by Conover's post-hoc analysis. All data are presented as mean \pm SEM (N=3).